

Experimentally Accessible Quantum Phase Transition in a non-Hermitian Tavis-Cummings Model Engineered with Two Drive Fields

Guo-Qiang Zhang,¹ Zhen Chen,^{1,2} and J. Q. You^{1,*}

¹*Interdisciplinary Center of Quantum Information, State Key Laboratory of Modern Optical Instrumentation, and Zhejiang Province Key Laboratory of Quantum Technology and Device, Department of Physics, Zhejiang University, Hangzhou 310027, China*

²*Quantum Physics and Quantum Information Division, Beijing Computational Science Research Center, Beijing 100193, China*

(Dated: September 1, 2022)

We study the quantum phase transition (QPT) in a non-Hermitian Tavis-Cummings (TC) model of experimentally accessible parameters, which is engineered with two drive fields applied to an ensemble of two-level systems (TLSs) and a cavity, respectively. When the two drive fields satisfy a given parameter-matching condition, the coupled cavity-TLS ensemble system can be described by an effective standard TC Hamiltonian in the rotating frame. In this ideal Hermitian case, the engineered TC model can exhibit the super-radiant QPT with spin conservation at an experimentally-accessible critical coupling strength, but the QPT is however spoiled by the decoherence. We find that in this non-Hermitian case, the QPT can be recovered by introducing a gain in the cavity to balance the loss of the TLS ensemble. Also, the spin-conservation law is found to be violated due to the decoherence of the system. Our study offers an experimentally realizable approach to implementing QPT in the non-Hermitian TC model.

Introduction.—Quantum phase transition (QPT) has been widely studied in various quantum systems (see, e.g., [1–12]), because of its fundamental importance in many-body physics and potential applications in quantum technologies [13]. Among them, the super-radiant QPT was predicted [14–17] in, e.g., the Dicke model [18], which involves the collective interaction between an ensemble of two-level systems (TLSs) and the quantized field in a cavity. In the thermodynamic limit of a large number of TLSs, the ground-state properties of the Dicke model, such as the excitations in the TLS ensemble, can display an abrupt change related to the QPT in the system [19–21], when continuously varying the collective coupling strength around a critical value. As required to be comparable to the frequencies of the TLS ensemble and the cavity mode, this critical coupling strength is difficult to achieve experimentally. Moreover, the no-go theorem due to the squared electromagnetic vector potential also hinders the presence of the super-radiant QPT in the Dicke model [22–24]. Due to these difficulties, the nonequilibrium QPT (i.e., the simulated QPT) has been proposed [25–27] and observed [28–30] in cavity quantum electrodynamics (QED) systems by engineering an effective Dicke Hamiltonian.

In the experiment, most quantum systems can only reach the strong-coupling regime [31, 32], where the Dicke model can be reasonably reduced to the Tavis-Cummings (TC) model [33] via the rotating-wave approximation (RWA) [34], i.e., ignoring the counter-rotating coupling terms between the TLS ensemble and the cavity mode. Similar to the Dicke model, the TC model is another archetypal model known to exhibit the super-radiant QPT [35]. Nevertheless, QPT in the TC model can occur only in the regime of extremely strong coupling, which is unaccessible for a realistic system and in which the RWA actually breaks down [34]. In addition, the decoherence inevitably occurring in the realistic system can spoil the QPT in the TC model [36–39]. Therefore, it is of

great importance to explore the nonequilibrium QPT by engineering an effective experimentally-accessible TC Hamiltonian [39–41].

In this Letter, we study the QPT in a driven quantum system consisting of a TLS ensemble coupled to a cavity mode. To reduce the critical coupling strength of the TC model, we use two external fields with the same frequency to drive the TLS ensemble and the cavity, respectively. By choosing proper drive-field parameters, an effective TC model can be rebuilt in the rotating frame, with the effective frequencies of the TLS ensemble and the cavity mode being their respective frequency detunings from the drive fields. In the ideal *Hermitian* case (i.e., without decoherence in the system), we can demonstrate the QPT in the driven system, where the corresponding critical coupling strength is tunable (via varying the drive-field frequency) and experimentally accessible. However, decoherence inevitably occurs in the system and the QPT of the TC model is spoiled in this *non-Hermitian* case [36–39]. We find that the QPT in the non-Hermitian TC model can be recovered by using a cavity with gain to *balance* the loss of the TLS ensemble. In sharp contrast to the spin conservation in the ideal Hermitian case, the spin-conservation law is found to be violated in the non-Hermitian case [42, 43]. Moreover, we propose to implement this non-Hermitian TC model with a hybrid circuit-QED system. To the best of our knowledge, this is the first proposal to engineer an experimentally accessible *non-Hermitian* TC model that can have QPT in the presence of decoherence in the system.

QPT in the ideal Hermitian case.—The proposed system consists of N TLSs (e.g., spins) in a cavity, each with the same transition frequency ω_s and coupled to a cavity mode with coupling strength λ_s [see Fig. 1(a)]. This system can be described in a RWA by the TC model (we set $\hbar = 1$)

$$H_{\text{TC}} = \omega_c a^\dagger a + \omega_s J_z + \frac{\lambda}{\sqrt{N}} (a^\dagger J_- + a J_+), \quad (1)$$

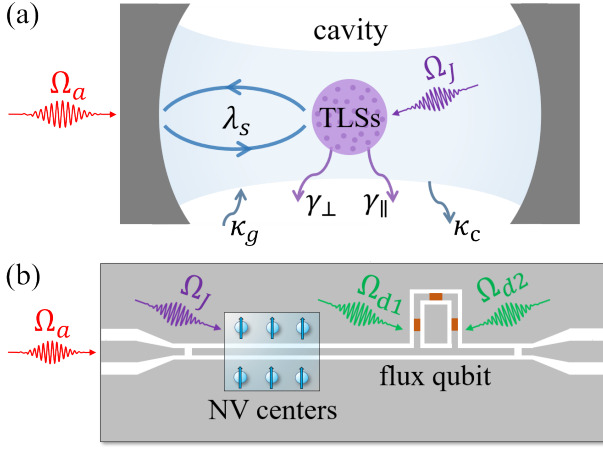


FIG. 1. (a) Schematic representation of the engineered TC model with a TLS ensemble strongly coupled to a cavity mode, where two drive fields with the same frequency are applied to the ensemble and the cavity mode, respectively. (b) Implementation of the proposed TC model using a hybrid circuit-QED system composed of an ensemble of NV centers in diamond interacting with an active coplanar-waveguide resonator, where the gain of the resonator results from an auxiliary flux qubit controlled by two microwave fields [49]. Also, two fields with the same frequency drive the NV ensemble and the resonator, respectively.

where a (a^\dagger) is the annihilation (creation) operator of the cavity mode with resonant frequency ω_c , J_x , J_y and J_z are the collective spin operators of the TLS ensemble with raising and lowering operators $J_\pm = J_x \pm iJ_y$, and $\lambda = \lambda_s \sqrt{N}$ is the collective coupling strength between the TLS ensemble and the cavity mode. This Hamiltonian has a conserved parity [35], $[H_{\text{TC}}, \Pi] = 0$, where $\Pi = \exp[i\pi(a^\dagger a + J_z + N/2)]$. In the ideal case without decoherence in the system, the TC model exhibits a QPT at the critical coupling strength $\lambda = \lambda_c \equiv \sqrt{\omega_s \omega_c}$ in the thermodynamic limit $N \rightarrow +\infty$ [35]. However, this QPT is spoiled by the decoherence of the system [36–39]. Also, it is extremely difficult to demonstrate the QPT due to the inaccessibility of the very large critical coupling strength λ_c in a realistic system.

To solve these problems, we first manage to reduce the critical coupling strength by applying two drive fields of the same frequency ω_d to the cavity and the TLS ensemble, respectively. This corresponds to adding the drive Hamiltonian $H_d = \Omega_a(a^\dagger e^{-i\omega_d t} + a e^{i\omega_d t}) + (\Omega_J/\sqrt{N})(J_+ e^{-i\omega_d t} + J_- e^{i\omega_d t})$ to the Hamiltonian in Eq. (1). Here Ω_a is the Rabi frequency between the drive field and the cavity mode, and $\Omega_J \equiv \Omega_s \sqrt{N}$ is the collective Rabi frequency between the drive field and the TLS ensemble, where Ω_s is the Rabi frequency between the drive field and each TLS. In a rotating reference frame with respect to the frequency ω_d of the two drive fields, the total Hamiltonian of the system can be converted to

$$H_{\text{TC}}^{(d)} = \Delta_c a^\dagger a + \Delta_s J_z + \frac{\lambda}{\sqrt{N}}(a J_+ + a^\dagger J_-) + (\Omega_a a^\dagger + \Omega_a^* a) + \frac{1}{\sqrt{N}}(\Omega_J J_+ + \Omega_J^* J_-), \quad (2)$$

where $\Delta_{c(s)} \equiv \omega_{c(s)} - \omega_d$ (> 0) is the frequency detuning of the cavity mode (TLS ensemble) relative to the corresponding drive field. By introducing a displacement $a = A + \alpha$ and $a^\dagger = A^\dagger + \alpha^*$ with $\alpha = -\Omega_a/\Delta_c$, i.e., a translation transform, the above Hamiltonian becomes

$$H_{\text{TC}}^{(d)} = \Delta_c A^\dagger A + \Delta_s J_z + \frac{\lambda}{\sqrt{N}}(A J_+ + A^\dagger J_-) + \frac{1}{\sqrt{N}}[(\Omega_J + \lambda\alpha)J_+ + (\Omega_J^* + \lambda\alpha^*)J_-], \quad (3)$$

where A^\dagger and A are also bosonic creation and annihilation operators obeying $[A, A^\dagger] = 1$. When the two drive fields satisfy the parameter-matching condition $\Omega_a/\Omega_J = \Delta_c/\lambda$, the effects of these two drive fields cancel each other and the Hamiltonian is reduced to

$$H_{\text{TC}}^{(d)} = \Delta_c A^\dagger A + \Delta_s J_z + \frac{\lambda}{\sqrt{N}}(A J_+ + A^\dagger J_-), \quad (4)$$

which has the same form as the standard TC model in Eq. (1), but the critical coupling strength $\lambda = \lambda_c \equiv \sqrt{\Delta_s \Delta_c}$ becomes experimentally accessible by reducing Δ_c (Δ_s) via tuning the drive-field frequency ω_d . Like the standard TC model in Eq. (1), the effective TC model in Eq. (4) also exhibits a normal (super-radiant) phase with unbroken (broken) parity symmetry when $\lambda < \lambda_c$ ($\lambda > \lambda_c$), and the TLS ensemble in the thermodynamic limit has the critical behaviors [41]

$$\frac{\langle J_z \rangle}{(N/2)} = \begin{cases} -1, & \lambda < \lambda_c; \\ -\lambda_c^2/\lambda^2, & \lambda \geq \lambda_c, \end{cases} \quad (5)$$

and

$$\frac{\langle J_- \rangle}{(N/2)} = \begin{cases} 0, & \lambda < \lambda_c; \\ (1 - \lambda_c^4/\lambda^4)^{1/2}, & \lambda \geq \lambda_c. \end{cases} \quad (6)$$

This gives $\langle J_z \rangle \sim |\lambda - \lambda_c|^{\nu_z}$ and $\langle J_- \rangle \sim |\lambda - \lambda_c|^{\nu_-}$ around $\lambda = \lambda_c$, with critical exponents $\nu_z = 1$ and $\nu_- = 1/2$. The displaced cavity field can also display a QPT because $\langle A \rangle = -\lambda \langle J_- \rangle / (\sqrt{N} \Delta_c)$, i.e., $\langle A^\dagger A \rangle$ behaves as $\langle A^\dagger A \rangle \sim |\lambda - \lambda_c|^{\nu_A}$, with $\nu_A = 1$. Therefore, $\langle a^\dagger a \rangle \sim |\lambda - \lambda_c|^{\nu_a}$, with $\nu_a = 1/2$ [44], owing to $\langle a \rangle \equiv \langle A \rangle + \alpha = -\lambda \langle J_- \rangle / (\sqrt{N} \Delta_c) - \Omega_a/\Delta_c$. Note that two suitable drive fields are required to demonstrate the QPT. If only one finite drive field is applied (i.e., either $\Omega_a \neq 0$ but $\Omega_J = 0$ or $\Omega_J \neq 0$ but $\Omega_a = 0$), the effective Hamiltonian of the driven system does not preserve the parity symmetry [45]. In this case, the system can only tend to exhibit the critical behavior when the sole drive field becomes extremely weak [41].

QPT in the non-Hermitian case with gain.—When the decoherence of the system is considered, the system becomes non-Hermitian. We use a Langevin equation approach [34] to study the critical behavior of the non-Hermitian system. With the Hamiltonian in Eq. (2), the dynamics of the driven system is governed by the following Langevin equations:

$$\dot{a} = -i(\Delta_c - i\kappa_c)a - i\frac{\lambda}{\sqrt{N}}J_- - i\Omega_a,$$

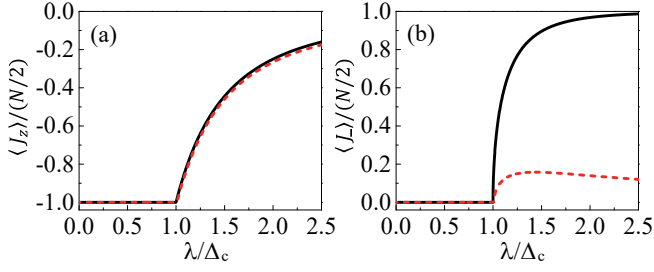


FIG. 2. (a) $\langle J_z \rangle / (N/2)$ and (b) $\langle J_- \rangle / (N/2)$ versus the reduced coupling strength λ/Δ_c under the parameter-matching condition of the two drive fields. For the (black) solid curve, $\kappa_c = \gamma_\perp = \gamma_\parallel = \kappa_g = 0$, while $\kappa_c = \gamma_\perp = 1$, $\gamma_\parallel = 0.1$ and $\kappa_g = \kappa_g^{(0)} = \kappa_c + \gamma_\perp \Delta_c / \Delta_s$ for the (red) dashed curve. Other parameters are $\lambda = 8$, $\Omega_a / \sqrt{N} = 1$, and $\Delta_s = \Delta_c$.

$$\begin{aligned} \dot{J}_- &= -i(\Delta_s - i\gamma_\perp)J_- + i\frac{2\lambda}{\sqrt{N}}J_z a + i2J_z \frac{\Omega_J}{\sqrt{N}}, \\ \dot{J}_z &= -i\frac{\lambda}{\sqrt{N}}(aJ_+ - a^\dagger J_-) - i\frac{1}{\sqrt{N}}(\Omega_J J_+ - \Omega_J^* J_-) - \gamma_\parallel \left(\frac{N}{2} + J_z\right), \end{aligned} \quad (7)$$

where κ_c is the decay rate of the cavity, and γ_\perp (γ_\parallel) is the transversal (longitudinal) relaxation rate of the TLS ensemble. The operator \mathcal{O} ($= \{a, J_-, J_z\}$) can be written as a sum of its expectation value $\langle \mathcal{O} \rangle$ and fluctuation $\delta\mathcal{O}$, i.e., $\mathcal{O} = \langle \mathcal{O} \rangle + \delta\mathcal{O}$. At the steady state $\langle \dot{\mathcal{O}} \rangle = 0$, it follows from Eq. (7) that

$$\begin{aligned} (\Delta_c - i\kappa_c)\langle a \rangle + \frac{\lambda}{\sqrt{N}}\langle J_- \rangle + \Omega_a &= 0, \\ (\Delta_s - i\gamma_\perp)\langle J_- \rangle - \frac{2\lambda}{\sqrt{N}}\langle J_z \rangle \langle a \rangle - 2\langle J_z \rangle \frac{\Omega_J}{\sqrt{N}} &= 0, \\ \frac{\lambda}{\sqrt{N}}(\langle a \rangle \langle J_+ \rangle - \langle a^\dagger \rangle \langle J_- \rangle) + \frac{1}{\sqrt{N}}(\Omega_J \langle J_+ \rangle - \Omega_J^* \langle J_- \rangle) \\ - i\gamma_\parallel \left(\frac{N}{2} + \langle J_z \rangle\right) &= 0, \end{aligned} \quad (8)$$

where a mean-field approximation is applied to the two-operator terms [46]. Substituting the first equation in Eq. (8) into the second and third equations in Eq. (8) to eliminate $\langle a \rangle$, we have

$$\begin{aligned} \left[1 + \frac{\lambda^2}{(\Delta_c \Delta_s - \kappa_c \gamma_\perp) - i(\Delta_c \gamma_\perp + \Delta_s \kappa_c)} \frac{\langle J_z \rangle}{(N/2)}\right] \langle J_- \rangle &= 0, \\ \frac{\kappa_c \lambda^2}{\Delta_c^2 + \kappa_c^2} \frac{\langle J_+ \rangle \langle J_- \rangle}{(N/2)^2} + \gamma_\parallel \left(1 + \frac{\langle J_z \rangle}{(N/2)}\right) &= 0, \end{aligned} \quad (9)$$

when the parameter-matching condition in the non-Hermitian case, $\Omega_a / \Omega_J = (\Delta_c - i\kappa_c) / \lambda$, is used. Obviously, Eq. (9) has only a set of *trivial* solutions $\langle J_z \rangle / (N/2) = -1$ and $\langle J_- \rangle = 0$. This verifies that the decoherence of the system ruins the QPT occurring in the standard Hermitian TC model [36–39].

To recover the QPT, we manage to introduce a gain medium in the dissipative cavity. With the gain included, we obtain the same equations as Eqs. (7)–(9), but κ_c is replaced by $\kappa \equiv \kappa_c - \kappa_g$, where κ_g is the gain rate of the cavity owing to the gain medium. The parameter-matching condition becomes

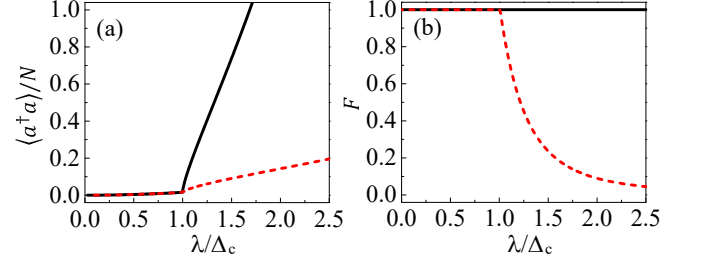


FIG. 3. (a) Mean photon number $\langle a^\dagger a \rangle / N$ and (b) characteristic quantity F of the TLS ensemble versus the reduced coupling strength λ/Δ_c , where $\kappa_c = \gamma_\perp = \gamma_\parallel = \kappa_g = 0$ for the (black) solid curve, and $\kappa_c = \gamma_\perp = 1$, $\gamma_\parallel = 0.1$ and $\kappa_g = \kappa_g^{(0)} = \kappa_c + \gamma_\perp \Delta_c / \Delta_s$ for the (red) dashed curve. Other parameters are the same as in Fig. 2.

$\Omega_a / \Omega_J = (\Delta_c - i\kappa) / \lambda$, and Eq. (9) is converted to

$$\begin{aligned} \left[1 + \frac{\lambda^2}{(\Delta_c \Delta_s - \kappa \gamma_\perp) - i(\Delta_c \gamma_\perp + \Delta_s \kappa)} \frac{\langle J_z \rangle}{(N/2)}\right] \langle J_- \rangle &= 0, \\ \frac{\kappa \lambda^2}{\Delta_c^2 + \kappa^2} \frac{\langle J_+ \rangle \langle J_- \rangle}{(N/2)^2} + \gamma_\parallel \left(1 + \frac{\langle J_z \rangle}{(N/2)}\right) &= 0. \end{aligned} \quad (10)$$

To have the QPT, we need $\Delta_c \gamma_\perp + \Delta_s \kappa \equiv \Delta_c \gamma_\perp - \Delta_s (\kappa_g - \kappa_c) = 0$, which gives the required gain rate $\kappa_g^{(0)} = \kappa_c + \gamma_\perp \Delta_c / \Delta_s$. Now, the parameter-matching condition $\Omega_a / \Omega_J = (\Delta_c - i\kappa) / \lambda$ is reduced to $\Omega_a / \Omega_J = \Delta_c (1 + i\gamma_\perp / \Delta_s) / \lambda$. When $\kappa_g = \kappa_g^{(0)}$, besides the set of trivial solutions $\langle J_z \rangle / (N/2) = -1$ and $\langle J_- \rangle = 0$, Eq. (10) has also another set of *nontrivial* solutions

$$\frac{\langle J_z \rangle}{(N/2)} = -\frac{\lambda_c^2}{\lambda^2}, \quad \frac{\langle J_- \rangle}{(N/2)} = \frac{\lambda_c}{\lambda} \left[\left(1 - \frac{\lambda_c^2}{\lambda^2}\right) \frac{\gamma_\parallel}{\gamma_\perp} \right]^{1/2}, \quad (11)$$

with λ_c modified as

$$\lambda_c \equiv \sqrt{\Delta_c \Delta_s (1 + \gamma_\perp^2 / \Delta_s^2)}. \quad (12)$$

Here $\langle J_- \rangle$ is assumed to be real for simplicity. As shown in Fig. 2, when varying the critical coupling strength λ_c from $\lambda < \lambda_c$ to $\lambda > \lambda_c$, the proposed driven system exhibits a QPT from the normal phase with $\langle J_z \rangle / (N/2) = -1$ and $\langle J_- \rangle = 0$ to the super-radiant phase with $\langle J_z \rangle$ and $\langle J_- \rangle$ given in Eq. (11). In the non-Hermitian case with gain, $\langle J_z \rangle / (N/2)$ has the same behavior as in the Hermitian case [see Fig. 2(a)]. In fact, around $\lambda = \lambda_c$, $\langle J_z \rangle \sim |\lambda - \lambda_c|^{\nu_z}$, with $\nu_z = 1$. Figure 2(b) shows that in the non-Hermitian case with gain, $\langle J_- \rangle / (N/2)$ is much reduced in the regime of super-radiant phase, but it can be analytically derived from Eq. (11) that around $\lambda = \lambda_c$, $\langle J_- \rangle / (N/2)$ still exhibits the same critical behavior as in the Hermitian case: $\langle J_- \rangle \sim |\lambda - \lambda_c|^{\nu_-}$, with $\nu_- = 1/2$.

From the first equation in Eq. (8), but with κ_c replaced by $\kappa = \kappa_c - \kappa_g^{(0)} = -\gamma_\perp \Delta_c / \Delta_s$, we have

$$\langle a \rangle = -\frac{\lambda}{\sqrt{N} \Delta_c (1 + i\gamma_\perp / \Delta_s)} \langle J_- \rangle - \frac{\Omega_a}{\Delta_c (1 + i\gamma_\perp / \Delta_s)}. \quad (13)$$

With $\gamma_\perp = 0$, it reduces to the result in the ideal Hermitian case. In Fig. 3(a), we plot $\langle a^\dagger a \rangle / N$ versus the reduced coupling strength λ/Δ_c in both the ideal Hermitian case and the

non-Hermitian case with gain. In these two cases, the results for $\langle a^\dagger a \rangle / N$ globally look different, but we can analytically derive that $\langle a^\dagger a \rangle / N$ in the non-Hermitian case with gain also exhibits the same critical behavior as in the Hermitian case, i.e., around $\lambda = \lambda_c$, $\langle a^\dagger a \rangle / N \sim |\lambda - \lambda_c|^{\nu_a}$, with $\nu_a = 1/2$ [44].

Without decoherence in the system ($\kappa_c = \gamma_\perp = \gamma_\parallel = 0$), $\Omega_a / \Omega_J = (\Delta_c - i\kappa_c) / \lambda$ is reduced to the parameter-matching condition in the ideal Hermitian case, $\Omega_a / \Omega_J = \Delta_c / \lambda$, and the second equation in Eq. (9) becomes trivial. In this Hermitian case, the results in Eqs. (5) and (6) are obtained by solving the first equation in Eq. (9) and using the spin-conservation law $\langle J_x \rangle^2 + \langle J_y \rangle^2 + \langle J_z \rangle^2 = (N/2)^2$ [38, 40]. In contrast, when the decoherence of the system is considered, the spin-conservation law is usually *violated*, with $\langle J_x \rangle^2 + \langle J_y \rangle^2 + \langle J_z \rangle^2 < (N/2)^2$ [42, 43]. To characterize this violation, we define a characteristic quantity $F = (\langle J_x \rangle^2 + \langle J_y \rangle^2 + \langle J_z \rangle^2) / (N/2)^2$. Obviously, $F = 1$ in the ideal Hermitian case owing to the spin-conservation law. For the non-Hermitian case with gain, it is easy to verify that $F = 1$ in the regime of normal phase, but

$$F = \frac{\lambda_c^2}{\lambda^2} \left(1 - \frac{\lambda_c^2}{\lambda^2} \right) \frac{\gamma_\parallel}{\gamma_\perp} + \frac{\lambda_c^4}{\lambda^4} \quad (14)$$

in the regime of super-radiant phase, where the ratio $\gamma_\parallel / \gamma_\perp$ between the longitudinal- and transversal-relaxation rates plays a significant role. In the non-Hermitian case with gain, F monotonically decreases when $\lambda / \Delta_c > 1.008$ (corresponding to $\lambda > \lambda_c$) [see the red dashed curve in Fig. 3(b)].

Possible implementation.—In the experiment, the proposed model with gain can be implemented using a hybrid circuit-QED system composed of a dissipative TLS ensemble, such as the nitrogen-vacancy (NV) centers in diamond, coupled to an active coplanar-waveguide resonator [see Fig. 1(b)]. The transition frequency of NV centers can be tuned by an external magnetic field and the number of NV centers in the sample can be $N \sim 10^{12}$ [47, 48], approaching the thermodynamic limit of the proposed system. The hybrid system is usually in the strong-coupling regime and can be described by a standard TC Hamiltonian in Eq. (1).

To engineer an active resonator, one can harness an auxiliary flux qubit transversely coupled to the resonator with a coupling strength g_a and longitudinally driven by two microwave fields [49]. After eliminating the degree of freedom of the auxiliary qubit, the effective gain rate κ_g of the resonator can be tuned from 0 to, e.g., $0.2g_a$ (i.e., $2\pi \times 6$ MHz for $g_a / 2\pi = 30$ MHz) by varying the amplitudes and frequencies of the two microwave fields [49]. Moreover, as shown in Fig. 1(b), two additional drive fields with Rabi frequencies Ω_a and Ω_J pump the NV-center ensemble and the resonator, respectively. When the parameter-matching condition $\Omega_a / \Omega_J = \Delta_c (1 + i\gamma_\perp / \Delta_s) / \lambda$ is achieved for these two drive fields, an experimentally accessible TC model is then engineered and the relevant quantities for demonstrating the QPT are governed by Eqs. (10) and (13).

Discussions and Conclusions.—The special case with only one drive field was studied in Refs. [41, 45], which is related to the cavity or the TLS ensemble pumped by a drive field,

i.e., Eq. (2) with $\Omega_a \neq 0$ but $\Omega_J = 0$ [41] or $\Omega_J \neq 0$ but $\Omega_a = 0$ [45]. At a finite strength of this drive field, the biased TC model does not preserve the parity symmetry due to the bias term and the QPT disappears in the system [45]. Only in the weak drive-field limit [i.e., either $\Omega_a \rightarrow 0$ when $\Omega_J = 0$ or $\Omega_J \rightarrow 0$ when $\Omega_a = 0$ in Eq. (2)] can the model tend to have the QPT [41]. For a realistic system, the cusplike QPT behavior is however much smoothed by the inevitable cavity loss and the dissipation of the TLS ensemble even in the weak drive-field limit [39]. In our proposal, when the two drive fields satisfy the parameter-matching condition, we can obtain an effective TC Hamiltonian with parity symmetry [i.e., Eq. (4)]. This TC Hamiltonian can exhibit QPT at an experimentally-accessible critical coupling strength and the weak drive-field limit is not necessary. Even with the decoherence of the system, the QPT behavior is still achievable by harnessing an active cavity (instead of a passive cavity). Very recently, the QPT in a TC model induced by a single *squeezed* drive field was investigated [40], where the effective Hamiltonian is a biased TC model with a two-photon drive term, corresponding to Eq. (2) with $\Omega_a a^\dagger + \Omega_a^* a$ replaced by $\Omega_a a^{\dagger 2} + \Omega_a^* a^2$ and $\Omega_J = 0$. Using a squeezing transformation, this biased TC Hamiltonian can be transformed to an anisotropic Dicke Hamiltonian [50]. Experimentally, if a *pure* squeezed drive field, $a^{\dagger 2} + a^2$, cannot be achieved, as discussed above, any finite *unsqueezed* part of the single drive field can ruin the QPT. In our study, the obtained effective Hamiltonian in Eq. (4) is a standard TC model without the bias term and no squeezed drive field is required. Also, the spin-conservation law is used in Ref. [40]. It is different from our non-Hermitian case in which the spin-conservation law is found to be violated [42, 43].

In conclusion, we have studied the QPT in a TC model engineered with two drive fields applied to the TLS ensemble and the cavity, respectively. In the ideal Hermitian case without decoherence, the QPT can occur at an experimentally-accessible critical coupling strength, but it is spoiled by the decoherence of the system. In this non-Hermitian case, we find that the QPT can be recovered by harnessing a gain in the cavity to balance the loss of the TLS ensemble. In sharp contrast to the spin conservation in the ideal Hermitian case, the spin-conservation law is however found to be violated in our non-Hermitian case. Moreover, we propose to implement this non-Hermitian TC model using a hybrid circuit-QED system. Our work provides an experimentally realizable approach to achieving QPT in the non-Hermitian TC model.

This work is supported by the National Key Research and Development Program of China (Grant No. 2016YFA0301200), the National Natural Science Foundation of China (Grants No. 11934010, No. U1801661, and No. 11774022).

* jqyou@zju.edu.cn

- [1] H. T. Mebrahtu, I. V. Borzenets, D. E. Liu, H. Zheng, Y. V. Bomze, A. I. Smirnov, H. U. Baranger, and G. Finkelstein, Quantum phase transition in a resonant level coupled to interacting leads, *Nature (London)* **488**, 61 (2012).
- [2] M. J. Hwang, R. Puebla, and M. B. Plenio, Quantum Phase Transition and Universal Dynamics in the Rabi Model, *Phys. Rev. Lett.* **115**, 180404 (2015).
- [3] M. J. Hwang and M. B. Plenio, Quantum Phase Transition in the Finite Jaynes-Cummings Lattice Systems, *Phys. Rev. Lett.* **117**, 123602 (2016).
- [4] Z. Zhou, D. Wang, Z. Y. Meng, Y. Wang, and C. Wu, Mott insulating states and quantum phase transitions of correlated $SU(2N)$ Dirac fermions, *Phys. Rev. B* **93**, 245157 (2016).
- [5] D. Wang, Y. Li, Z. Cai, Z. Zhou, Y. Wang, and C. Wu, Competing Orders in the 2D Half-Filled $SU(2N)$ Hubbard Model through the Pinning-Field Quantum Monte Carlo Simulations, *Phys. Rev. Lett.* **112**, 156403 (2014).
- [6] A. Aharony and A. B. Harris, Absence of Self-Averaging and Universal Fluctuations in Random Systems near Critical Points, *Phys. Rev. Lett.* **77**, 3700 (1996).
- [7] S. Sachdev and J. Ye, Gapless spin-fluid ground state in a random quantum Heisenberg magnet, *Phys. Rev. Lett.* **70**, 3339 (1993).
- [8] A. B. Harris, A. Aharony, and O. Entin-Wohlman, Order Parameters and Phase Diagram of Multiferroic RMn_2O_5 , *Phys. Rev. Lett.* **100**, 217202 (2008).
- [9] J. Zhang, C. Z. Chang, P. Tang, Z. Zhang, X. Feng, K. Li, L. Wang, X. Chen, C. Liu, W. Duan, K. He, Q. K. Xue, X. Ma, and Y. Wang, Topology-Driven Magnetic Quantum Phase Transition in Topological Insulators, *Science* **339**, 1582 (2013).
- [10] D. Zhang, X. Q. Luo, Y. P. Wang, T. F. Li, and J. Q. You, Observation of the exceptional point in cavity magnon-polaritons, *Nat. Commun.* **8**, 1368 (2017).
- [11] X. Y. Lü, L. L. Zheng, G. L. Zhu, and Y. Wu, Single-Photon-Triggered Quantum Phase Transition, *Phys. Rev. Appl.* **9**, 064006 (2018).
- [12] Y. C. He and Y. Chen, Distinct Spin Liquids and Their Transitions in Spin-1/2 XXZ Kagome Antiferromagnets, *Phys. Rev. Lett.* **114**, 037201 (2015).
- [13] S. Sachdev, *Quantum Phase Transitions*, 2nd ed. (Cambridge University Press, Cambridge, England, 2011).
- [14] K. Hepp and E. H. Lieb, On the superradiant phase transition for molecules in a quantized radiation field: the Dicke maser model, *Ann. Phys. (N.Y.)* **76**, 360 (1973).
- [15] Y. K. Wang and F. T. Hioe, Phase Transition in the Dicke Model of Superradiance, *Phys. Rev. A* **7**, 831 (1973).
- [16] F. T. Hioe, Phase Transitions in Some Generalized Dicke Models of Superradiance, *Phys. Rev. A* **8**, 1440 (1973).
- [17] K. Hepp and E. H. Lieb, Equilibrium Statistical Mechanics of Matter Interacting with the Quantized Radiation Field, *Phys. Rev. A* **8**, 2517 (1973).
- [18] R. H. Dicke, Coherence in Spontaneous Radiation Processes, *Phys. Rev.* **93**, 99 (1954).
- [19] C. Emary and T. Brandes, Quantum Chaos Triggered by Precursors of a Quantum Phase Transition: The Dicke Model, *Phys. Rev. Lett.* **90**, 044101 (2003).
- [20] C. Emary and T. Brandes, Chaos and the quantum phase transition in the Dicke model, *Phys. Rev. E* **67**, 066203 (2003).
- [21] J. Ye and C. L. Zhang, Superradiance, Berry phase, photon phase diffusion, and number squeezed state in the $U(1)$ Dicke (Tavis-Cummings) model, *Phys. Rev. A* **84**, 023840 (2011).
- [22] K. Rzażewski, K. Wódkiewicz, and W. Żakowicz, Phase Transitions, Two-Level Atoms, and the A^2 Term, *Phys. Rev. Lett.* **35**, 432 (1975).
- [23] I. Bialynicki-Birula and K. Rzażewski, No-go theorem concerning the superradiant phase transition in atomic systems, *Phys. Rev. A* **19**, 301 (1979).
- [24] T. Jaako, Z. L. Xiang, J. J. Garcia-Ripoll, and P. Rabl, Ultrastrong-coupling phenomena beyond the Dicke model, *Phys. Rev. A* **94**, 033850 (2016).
- [25] F. Dimer, B. Estienne, A. S. Parkins, and H. J. Carmichael, Proposed realization of the Dicke-model quantum phase transition in an optical cavity QED system, *Phys. Rev. A* **75**, 013804 (2007).
- [26] D. Nagy, G. Kónya, G. Szirmai, and P. Domokos, Dicke-Model Phase Transition in the Quantum Motion of a Bose-Einstein Condensate in an Optical Cavity, *Phys. Rev. Lett.* **104**, 130401 (2010).
- [27] L. J. Zou, D. Marcos, S. Diehl, S. Putz, J. Schmiedmayer, J. Majer, and P. Rabl, Implementation of the Dicke Lattice Model in Hybrid Quantum System Arrays, *Phys. Rev. Lett.* **113**, 023603 (2014).
- [28] K. Baumann, C. Guerlin, F. Brennecke, and T. Esslinger, Dicke quantum phase transition with a superfluid gas in an optical cavity, *Nature (London)* **464**, 1301 (2010).
- [29] K. Baumann, R. Mottl, F. Brennecke, and T. Esslinger, Exploring Symmetry Breaking at the Dicke Quantum Phase Transition, *Phys. Rev. Lett.* **107**, 140402 (2011).
- [30] M. P. Baden, K. J. Arnold, A. L. Grimsmo, S. Parkins, and M. D. Barrett, Realization of the Dicke Model Using Cavity-Assisted Raman Transitions, *Phys. Rev. Lett.* **113**, 020408 (2014).
- [31] Z. L. Xiang, S. Ashhab, J. Q. You, and F. Nori, Hybrid quantum circuits: Superconducting circuits interacting with other quantum systems, *Rev. Mod. Phys.* **85**, 623 (2013).
- [32] G. Kurizki, P. Bertet, Y. Kubo, K. Mølmer, D. Petrosyan, P. Rabl, and J. Schmiedmayer, Quantum technologies with hybrid systems, *Proc. Natl. Acad. Sci. USA* **112**, 3866 (2015).
- [33] M. Tavis and F. W. Cummings, Exact Solution for an N -Molecule-Radiation-Field Hamiltonian, *Phys. Rev.* **170**, 379 (1968).
- [34] D. F. Walls and G. J. Milburn, *Quantum Optics* (Springer, Berlin, 1994).
- [35] O. Castañón, R. López-Peña, E. Nahmad-Achar, J. G. Hirsch, E. López-Moreno, and J. E. Vitela, Coherent state description of the ground state in the Tavis-Cummings model and its quantum phase transitions, *Phys. Scr.* **79**, 065405 (2009).
- [36] J. Keeling, M. J. Bhaseen, and B. D. Simons, Collective Dynamics of Bose-Einstein Condensates in Optical Cavities, *Phys. Rev. Lett.* **105**, 043001 (2010).
- [37] J. Larson and E. K. Irish, Some remarks on superradiant phase transitions in light-matter systems, *J. Phys. A* **50**, 174002 (2017).
- [38] M. Soriente, T. Donner, R. Chitra, and O. Zilberberg, Dissipation-Induced Anomalous Multicritical Phenomena, *Phys. Rev. Lett.* **120**, 183603 (2018).
- [39] M. Feng, Y. P. Zhong, T. Liu, L. L. Yan, W. L. Yang, J. Twamley, and H. Wang, Exploring the quantum critical behaviour in a driven Tavis-Cummings circuit, *Nat. Commun.* **6**, 7111 (2015).
- [40] C. J. Zhu, L. L. Ping, Y. P. Yang, and G. S. Agarwal, Squeezed Light Induced Symmetry Breaking Superradiant Phase Transition, *Phys. Rev. Lett.* **124**, 073602 (2020).
- [41] J. H. Zou, T. Liu, M. Feng, W. L. Yang, C. Y. Chen, and J. Twamley, Quantum phase transition in a driven Tavis-Cummings model, *New J. Phys.* **15**, 123032 (2013).
- [42] E. G. D. Torre, Y. Shchadilova, E. Y. Wilner, M. D. Lukin, and E. Demler, Dicke phase transition without total spin conserva-

- tion, Phys. Rev. A **94**, 061802 (2016).
- [43] P. Kirton and J. Keeling, Suppressing and Restoring the Dicke Superradiance Transition by Dephasing and Decay, Phys. Rev. Lett. **118**, 123602 (2017).
- [44] See Supplemental Materials.
- [45] C. Emary and T. Brandes, Phase transitions in generalized spin-boson (Dicke) models, Phys. Rev. A **69**, 053804 (2004).
- [46] D. O. Krimer, M. Zens, and S. Rotter, Critical phenomena and nonlinear dynamics in a spin ensemble strongly coupled to a cavity. I. Semiclassical approach, Phys. Rev. A **100**, 013855 (2019).
- [47] Y. Kubo, F. R. Ong, P. Bertet, D. Vion, V. Jacques, D. Zheng, A. Dréau, J. F. Roch, A. Auffeves, F. Jelezko, J. Wrachtrup, M. F. Barthe, P. Bergonzo, and D. Esteve, Strong Coupling of a Spin Ensemble to a Superconducting Resonator, Phys. Rev. Lett. **105**, 140502 (2010).
- [48] R. Amsüss, C. Koller, T. Nöbauer, S. Putz, S. Rotter, K. Sandner, S. Schneider, M. Schramböck, G. Steinhauser, H. Ritsch, J. Schmiedmayer, and J. Majer, Cavity QED with Magnetically Coupled Collective Spin States, Phys. Rev. Lett. **107**, 060502 (2011).
- [49] F. Quijandría, U. Naether, S. K. Özdemir, F. Nori, and D. Zueco, \mathcal{PT} -symmetric circuit QED, Phys. Rev. A **97**, 053846 (2018).
- [50] W. Qin, A. Miranowicz, P. B. Li, X. Y. Lü, J. Q. You, and F. Nori, Exponentially Enhanced Light-Matter Interaction, Cooperativities, and Steady-State Entanglement Using Parametric Amplification, Phys. Rev. Lett. **120**, 093601 (2018).